Characterizing neural activities evoked by manual acupuncture through spiking irregularity measures*

Xue Ming(薛 明), Wang Jiang(王 江)†, Deng Bin(邓 斌),
Wei Xi-Le(魏熙乐), Yu Hai-Tao(于海涛), and Chen Ying-Yuan(陈颖源)

School of Electrical Engineering and Automation, Tianjin University, Tianjin 300072, *China*

(Received 19 February 2013; revised manuscript received 22 March 2013)

The neural system characterizes information in external stimulations by different spiking patterns. In order to examine how neural spiking patterns are related to acupuncture manipulations, experiments are designed in such a way that different types of manual acupuncture (MA) manipulations are taken at the 'Zusanli' point of experimental rats, and the induced electrical signals in the spinal dorsal root ganglion are detected and recorded. The interspike interval (ISI) statistical histogram is fitted by the gamma distribution, which has two parameters: one is the time-dependent firing rate and the other is a shape parameter characterizing the spiking irregularities. The shape parameter is the measure of spiking irregularities and can be used to identify the type of MA manipulations. The coefficient of variation is mostly used to measure the spike time irregularity, but it overestimates the irregularity in the case of pronounced firing rate changes. However, experiments show that each acupuncture manipulation will lead to changes in the firing rate. So we combine four relatively rate-independent measures to study the irregularity of spike trains evoked by different types of MA manipulations. Results suggest that the MA manipulations possess unique spiking statistics and characteristics and can be distinguished according to the spiking irregularity measures. These studies have offered new insights into the coding processes and information transfer of acupuncture.

Keywords: acupuncture, interspike interval, gamma distribution, spiking irregularity measure

PACS: 87.19.ls, 87.19.lt, 87.85.Ng **DOI:** 10.1088/1674-1056/22/9/098703

1. Introduction

Acupuncture is a key component of traditional Chinese medicine (TCM). Current scientific research supports the efficacy of acupuncture for the treatment of some diseases,[1–3] especially in the relief of certain types of pain and post-operative nausea.[4–7] It has been shown that acupuncture evokes nervous system, neurotransmitter, and endogenous substance responses [8–12] and has underlying molecular effect mechanisms.[13,14] However, the underlying mechanisms of acupuncture are still unclear, and the reason why different types of manual acupuncture (MA) have different effects has not been found.

"Zusanli" is the most intensively studied single point treatment in acumoxa therapy.[15,16] It is located below the knee, on the anterior tibialis muscle (see Fig. 1(a)). Acupuncture is a mechanical stimulation. When the nociceptors whose receptive fields are distributed at the Zusanli point respond to the acupuncture stimulus, action potentials are initiated at the tip of the peripheral branch, i.e., the dorsal root ganglion cell (see Fig. 1(b)).[17] These action potentials are conducted downward the axon and enter into the central branch that innervates the second-order neurons in the spinal cord or in the medulla.[17]

Neural electrical signals evoked by MA manipulations have been characterized by nonlinear data analysis[18,19] and complex network mapping.[20] Types of acupuncture manipulations performed on rats have been inferred by the Bayesian decoding algorithm.[21] A delayed feedforward network model with plasticity has been established for investigating the acupuncture signal transmission path.[22] Electroencephalography (EEG) signals induced by acupuncture have also been studied based on complexity analysis and mutual information Lempel–Ziv complexity.[23–26] However, methods for recognizing the firing patterns of different MAs efficiently have not been found. Therefore, in this paper, the irregularities of different acupuncture electrical signals are computed based on a statistical model of interspike interval (ISI) sequences to identify the MA manipulations.

The ISI sequences of the neural spike train are always used to investigate the neural coding.[27–31] An interspike interval histogram (ISIH) is defined as the distribution of intervals of different lengths.[32] A number of statistical distributions have been used to describe various ISIHs, including the gamma,[33] the inverse Gaussian, the Weibull,[34] and the Lognormal[35] distributions. The gamma model is specified by two parameters: a time-dependent rate parameter and a shape parameter related to the spiking irregularity.[36] In this paper, the ISIH is fitted with the gamma distribution because the spiking irregularity measure can be used to characterize and distinguish the MA manipulations.

*Project supported by the National Natural Science Foundation of China (Grant Nos. 61072012 and 61172009), the Young Scientists Fund of the National Natural Science Foundation of China (Grant No. 61104032), and the China Postdoctoral Science Foundation (Grant No. 2012M510750).

†Corresponding author. E-mail: jiangwang@tju.edu.cn

© 2013 Chinese Physical Society and IOP Publishing Ltd

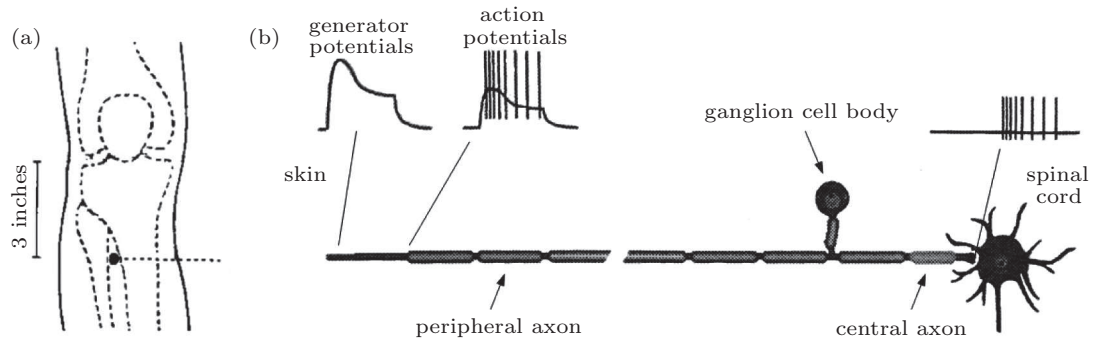


Fig. 1. Schematic diagram of acupuncture effect mechanism: (a) Zusanli acupoint; (b) the initiation and transmission of action potentials in the dorsal root ganglion.

It is thought that irregularity indicates the presence of temporal coding.[37–41] The classical measure of spiking irregularity is the coefficient of variation ($C_{\rm V}$), which is a global measure defined as the dispersion of the ISI sequence.[42] However, the irregularity of firing is largely overestimated by the $C_{\rm V}$ in the case of significant changes in firing rate. Then, alternative measures of irregularity are proposed, and it is demonstrated that they are local in time and therefore relatively independent of rate changes. Here four local spiking irregularity measures are used together to investigate the acupuncture electrical signals in this paper: the measure spiking irregularity $S_{\rm I}$,[40] the local variation $L_{\rm V}$,[43–45] the local coefficient of variation $C_{\rm V2}$,[46] and the average metric of ISI sequence $I_{\rm R}$.[40]

The remainder of this paper is structured as follows. In Section 2, the animal acupuncture experiments are designed and the neural electrical signals are recorded and preprocessed. In Section 3, the ISIH is fitted with the gamma distribution and the spiking irregularity measures are computed. Finally, the discussion and conclusion are given.

2. Signal acquisition and preprocessing

2.1. Design of the acupuncture experiment

The data come from healthy adult Sprague Dawley rats (200–300 g) anesthetized deeply by 20% ethyl carbamate (1.5 g/kg). After dissecting the rat to expose the lumbar nucleus, nerve tracts in L4 spinal root, pseudo-unipolar neurons whose receptive fields are located in the Zusanli point area are found in the spinal dorsal root. To reveal the effects of MAs of different types, the acupuncture electrical signals are recorded from pseudo-unipolar neurons when TB, TX, NB, and NX MA manipulations are taken at the Zusanli point of experimental rats for 90–120 times periodically within 2 min. Here, the TB and TX manipulations belong to the lifting and thrusting type, while the NB and NX manipulations belong to the twisting type. This procedure is designed according to the timing when acupuncture is used in clinical treatments. In order to ensure the accuracy of coding to acupuncture, the acupuncture needle is kept in the skin during the whole experiment. The electrical signals are detected by platinum electrodes and recorded by MP150 (BIOPAC), and the sampling frequency of the signals is 40 kHz. Meanwhile, the acupuncture times are recorded in the process of the experiment. Considering the adaption of neurons to the acupuncture stimulus, we eliminate the data induced by the acupuncture for the first 10 times. Manipulations are stopped for 5 min between different patterns of MAs to eliminate the effects of the previous MA. The data come from experiments on 7 rats, and all experiments on one rat are regarded as one session.

2.2. Data preprocessing

The neural spike activity evoked by acupuncture is recorded as continuous wide-band data in the spinal dorsal root ganglion, so spike detection and sorting should be accomplished first[47] to obtain the spike train of an individual pseudo-unipolar neuron. After band-filtering the data between 300 Hz and 3000 Hz, the spikes are detected by setting the threshold at

$$x_{\rm th} = 3\sigma, \quad \sigma = \text{median}\{|x|/0.6745\}, \tag{1}$$

where x is the signal after band-filtering and σ is the estimate of the standard deviation of the noise. The interference of the spikes is diminished by using the estimation based on the median value instead of the standard deviation of the filtered signal.[47] A time series after band-filtering is shown in Fig. 2(a).

After the detection of spikes, the features of the spike shapes are extracted by the wavelet transform as the inputs to the clustering algorithm. Then the superparamagnetic clustering (SPC) algorithm[47] is used to assign spikes with similar shapes to one cluster. After spike-detecting and spike-sorting, the spikes are assigned to two clusters based on their spike shapes as shown in Fig. 2(b). Different types of spike shapes are classified into different areas according to their wavelet coefficients. There are two separate areas in the plane of two wavelet coefficients, as shown in Fig. 2(c). Therefore the spike shapes can be classified into two clusters. Very few spontaneous spikes can be observed if the acupuncture needle in the skin remains stationary. Each acupuncture stimulus evokes an obvious bursting, which contains the main information about the acupuncture encoded by the pseudo-unipolar neuron. The bursting of the neurons leads to pronounced changes in the firing rate, so we can use the local spiking irregularity measure instead of the global measure to investigate the acupuncture spike trains.

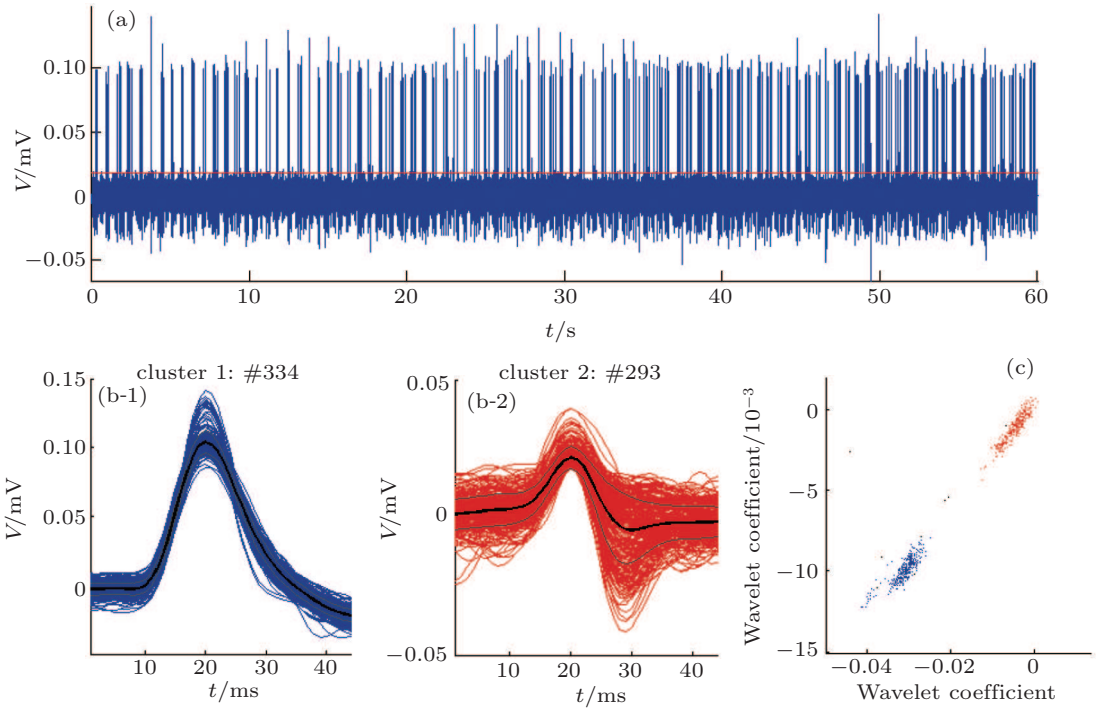


Fig. 2. (color online) Spike-sorting of signals detected in spinal cord dorsal root: (a) signals after band-filtering between 300 Hz and 3000 Hz; (b) spike shapes of neuronal clusters; (c) distribution of wavelet coefficients.

2.3. Interspike interval

The ISI sequence of biological firing is the basic method for studying the neural electrical signal coding. An ISI is defined as the time interval between two adjacent spike peaks, as shown in Fig. 3. An ISI sequence is presented as $T(n)$, $(n = 1,\ldots,N)$. The length of ISI obtained from dorsal root electrical signals depends on the type and the frequency of the MA. Figure 4 shows the diagrams of the ISI sequences for four MA manipulations.[19] It can be seen that the number of ISIs for each MA manipulation is quite different and the distributions of the ISI values are also different.

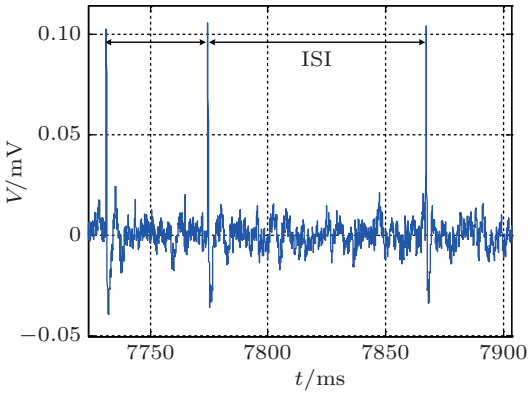


Fig. 3. (color online) Schematic diagram of the ISI.

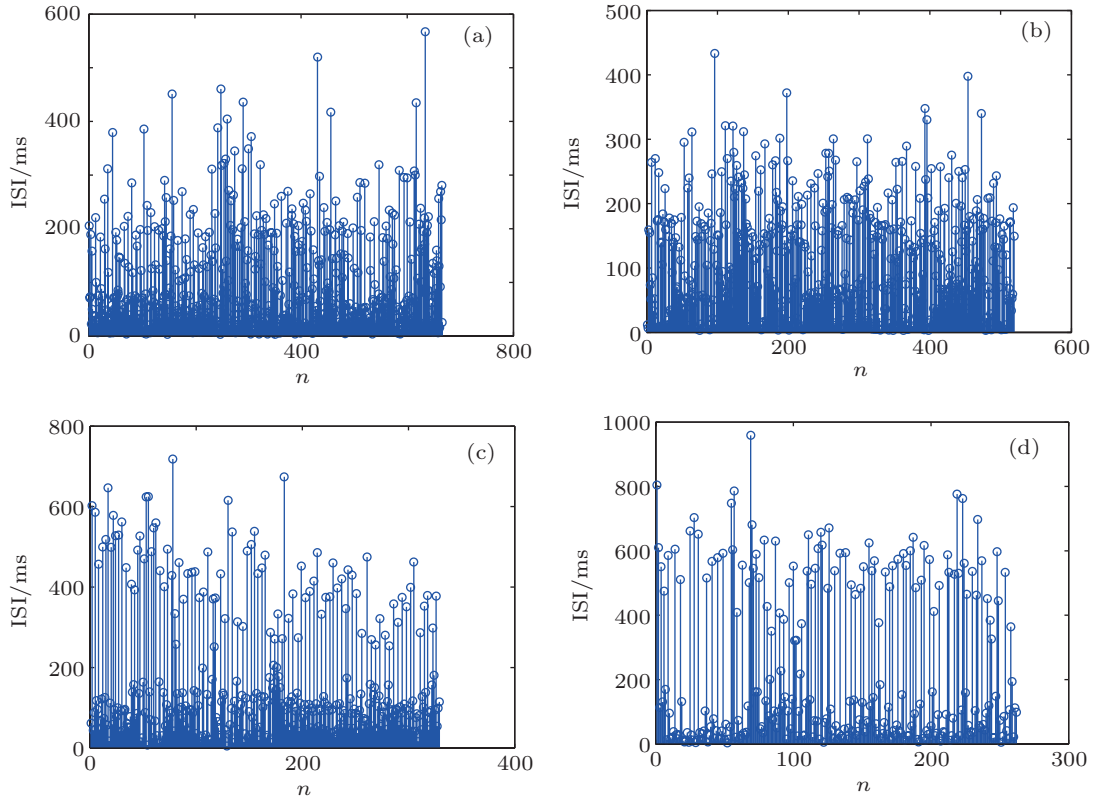


Fig. 4. (color online) ISI sequences of neural spike activities evoked by four MA manipulations: (a) TB; (b) TX; (c) NB; (d) NX.

3. Analysis methods and results

3.1. Distribution of ISI and gamma fitting

The ISIH represents the distribution of intervals of different lengths.[48] The distribution that parametrically represents the mean ISI and the mean ln(ISI) is the gamma distribution, which has frequently been adopted in neuroscience.[33,49,50] A gamma process is a better representation of a neuron spike train than a Poisson process, since it takes the effect of a relatively refractory period into account.[49,51] The gamma distribution is also derived as the optimal ISI distribution under the energy constraint.[52]

The gamma distribution gives the probability of finding an interspike interval T, and has two parameters, rate r and shape parameter α (sometimes called the gamma order), which are independently varied.[40] The form of the gamma distribution is given by

$$q(T;r,\alpha) = \frac{(\alpha r)^{\alpha}}{\Gamma(\alpha)} T^{\alpha-1} \mathrm{e}^{-\alpha r T}, \tag{2}$$

where the random variable T denotes an ISI and $\Gamma(\alpha)$ is the gamma function. Thus, with this model, it is possible to vary the irregularity by manipulating α. In many studies, the gamma process is fitted to the experimental data.[33]

The mean and variance of the ISI sequence are

$$\mathrm{Ex}(T) = \frac{1}{r}, \quad \mathrm{Var}(T) = \frac{1}{r^2\alpha}, \tag{3}$$

where r is the mean firing rate and α is the shape parameter. The $\alpha = 1$ corresponds to a Poisson process in which the instantaneous firing rate is constant over time independent of the previous firing time. In this case, a spike train looks irregular. When α is large, a gamma distribution can be approximated by a normal distribution, whose variance decreases with α increasing. In the limit of large α, the ISI becomes completely regular. The gamma processes with the shape parameter α being larger than, equal to, and smaller than unity generate firing patterns termed regular, random (Poisson), and bursty, respectively.[40,45,53] Thus, α is related to the spiking irregularity.

The ISIH and the gamma fittings for the four types of MA manipulations are shown in Fig. 5. It is found that the underlying distribution of the ISIs can be exactly fitted by the gamma distribution. The differences in gamma distribution among different types of MA manipulations show that the shape parameter charactering the spiking irregularity can be used to distinguish the MA manipulations. Therefore, we will combine the four different irregularity measures together to investigate the differences among the MA manipulations in the following subsections.

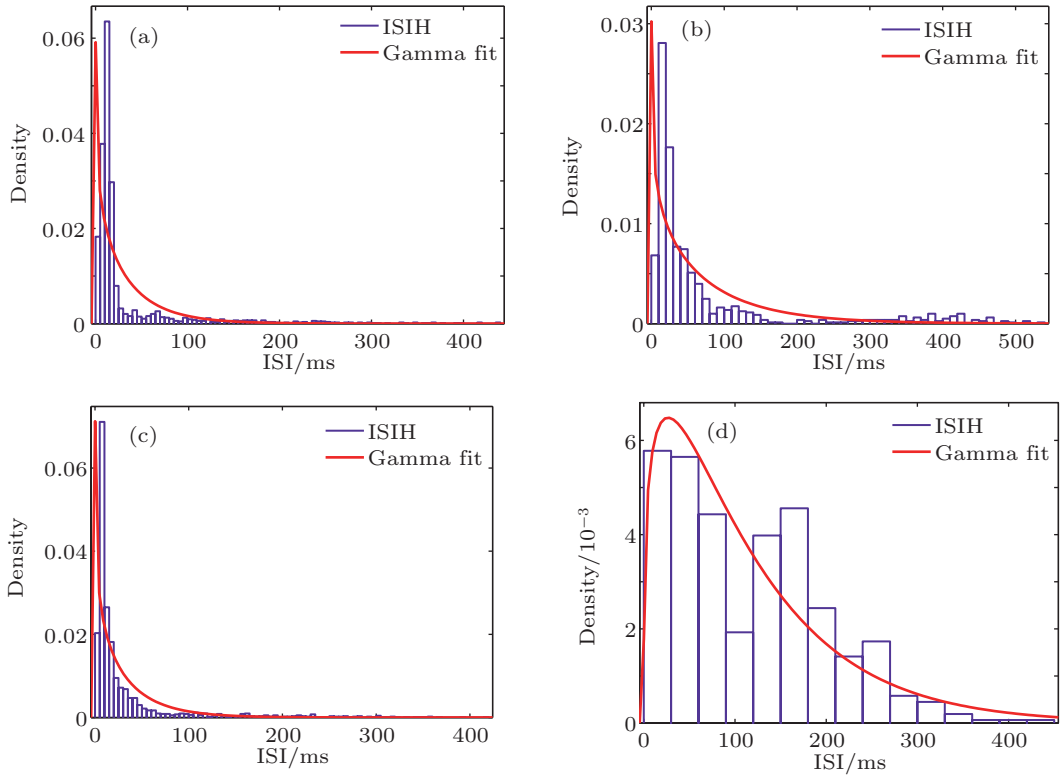


Fig. 5. (color online) Gamma distribution fittings of ISIH for four MA manipulations: (a) TB; (b) TX; (c) NB; (d) NX.

3.2. Measure of spiking irregularity S_{I}

The spiking irregularity S_{I} enables one to estimate optimally the shape parameter of a spike train under a gamma-distributed assumption of spiking activity.[36] The measure of S_{I} is an estimator of α, relatively independent of the firing rate change. For these reasons, S_{I} is suggested for use as a measure of spiking irregularity. The metric S_{I} is determined as follows:

$$S_{\mathrm{I}} = -\frac{1}{1-\ln(2)}\frac{1}{2N}\sum_{i=1}^{N}\ln\left(\frac{4T_iT_{i+1}}{(T_i+T_{i+1})^2}\right), \tag{4}$$

where T_i is an ISI. The normalization factor $1-\ln(2)$ is chosen for obtaining $S_{\mathrm{I}} = 1$ for a Poisson process to fall in the same range as the classical C_{V}.

Figure 6(a) shows the values of spiking irregularity S_{I} for the neural activities evoked by four MA manipulations. In order to facilitate the comparison between the different groups of experiments, we normalize each session of the results, i.e., we process matrices by transforming the mean and the standard deviation of each row to 0 and 1, respectively (as shown in Fig. 8(b)). Figure 8(b) shows a clear distinction between different MA manipulations after the normalization.

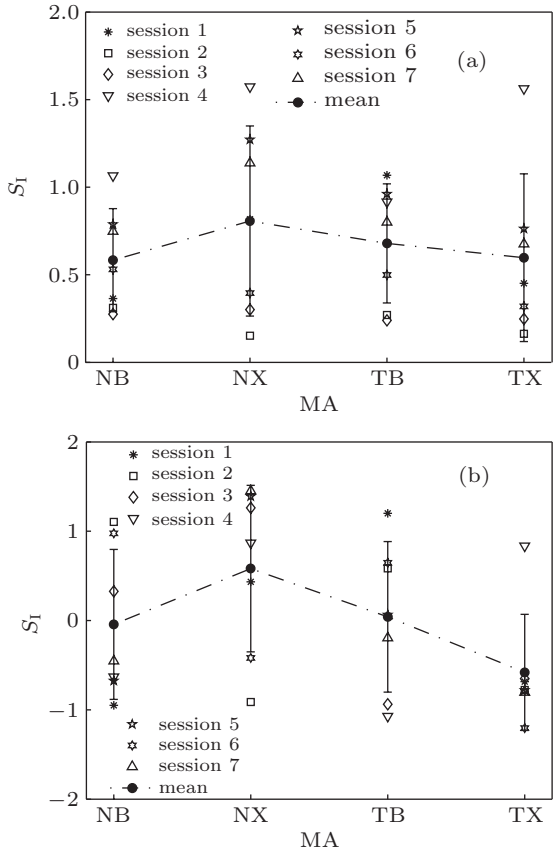


Fig. 6. Statistical analyses of the spiking irregularity measure S_{I} for the four MA manipulations (7 sessions): (a) original spiking irregularity measure S_{I}; (b) normalized spiking irregularity measure S_{I}.

3.3. Measure of spiking irregularity L_V

The L_V measure reflects the stepwise variability of the ISI sequence and extracts the spiking characteristics effectively, even for cases in which the spike rate is externally modulated.[44] It is also confirmed that for the rate modulated gamma process, the value of L_V does not undergo large changes due to the rate fluctuation, but is mainly determined by the form of the intrinsic ISI distribution parameterized by the shape parameter of a gamma distribution.

We can analytically obtain L_V for the gamma process in which the ISIs are derived from the gamma distribution of the shape parameter α. The L_V can be obtained as $L_V = 3/(2\alpha+1)$, i.e., α can also be estimated by using L_V.[44,46,54] The local variation of ISI is defined as

$$L_V = \frac{1}{N}\sum_{i=1}^{N} 3\frac{(T_i - T_{i+1})^2}{(T_i + T_{i+1})^2}, \tag{5}$$

where T_i is an ISI. Here, the summand is proportional to the square of the individual term $C_{V2} = 2|T_i - T_{i+1}|/|T_i + T_{i+1}|$,[45] which will be introduced in the next subsection. When a series of intervals is independently exponentially distributed, L_V is expected to take the value of 1. For a regular spike sequence in which T_i is a constant, L_V takes the value of 0.[44]

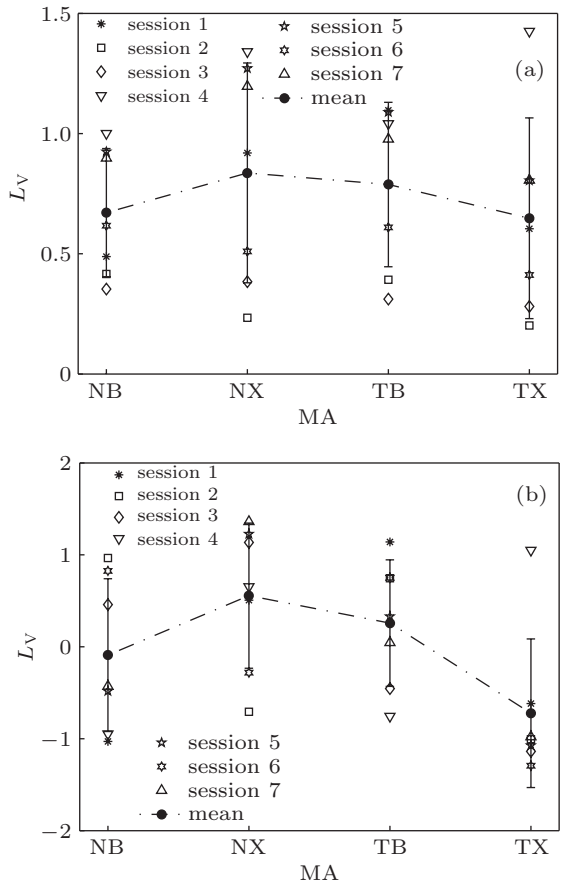


Fig. 7. Statistical analyses of the spiking irregularity measure L_V for the four MA manipulations (7 sessions): (a) original spiking irregularity measure L_V; (b) normalized spiking irregularity measure L_V.

In fact, there exists a tight inequality between S_I and L_V. By using Jensen's inequality, we have

$$\begin{aligned} S_I &= -\frac{1}{2N}\sum_{i=1}^{N} \ln\left(\frac{4T_iT_{i+1}}{(T_i+T_{i+1})^2}\right) \\ &\geq -\frac{1}{2}\ln\left(\frac{1}{N}\sum_{i=1}^{N}\frac{4T_iT_{i+1}}{(T_i+T_{i+1})^2}\right) \\ &= -\frac{1}{2}\ln\left(1-\frac{L_V}{3}\right). \end{aligned} \tag{6}$$

Thus, L_V gives a lower bound of S_I. Since S_I and α are inversely related, L_V gives an upper bound on α. This relation may be useful when only the value of L_V is available. Note that this relation holds for any spike trains independent of their statistical models and for any N.[36]

Figure 7 shows the L_V values of spiking irregularity for the neural activities evoked by four MA manipulations. The irregularity of the NX manipulation is higher than the NB and NX manipulations and the TX manipulation is obviously lower than the NB and NX manipulations. So the NX manipulation can clearly be distinguished from the TX manipulation according to the irregularity.

3.4. Measure of spiking irregularity C_{V2}

By calculating the statistics of the measures in the case of gamma-distributed spike trains, it has been demonstrated that C_{V2} is the measure with the lowest variance in the four local measures and induces the least errors when the number of ISIs in each window is limited and the firing rate changes are abrupt.[42] For these reasons, C_{V2} is the most suitable measure for a time-resolved analysis.

The metric C_{V2} of spiking irregularity is defined as follows:

$$C_{V2} = \frac{1}{N}\sum_{i=1}^{N} 2\frac{|T_i - T_{i+1}|}{T_i + T_{i+1}}, \tag{7}$$

where T_i is an ISI. The expected value of C_{V2} for a gamma process is given as

$$C_{V2}(\alpha) = \frac{4^{-\alpha+1}}{\alpha}\frac{\Gamma(2\alpha)}{\Gamma(\alpha)^2}, \tag{8}$$

where $\Gamma(\alpha)$ is the gamma function. The C_{V2} will be high for a spike train with a high interval-to-interval variability, but it will be lower for a spike train in which the variation occurs on the time scale much longer than the typical ISI value. The C_{V2} is more powerful in comparing the temporal ISI randomness of the spike train.

Figure 8 shows the C_{V2} values of spiking irregularity for the neural activities evoked by four MA manipulations. The difference in irregularity between the NX and TB manipulations is relatively small. The means of the irregularity for NB and TX manipulations are all negative and they can be obviously distinguished from the NX and TB manipulations.

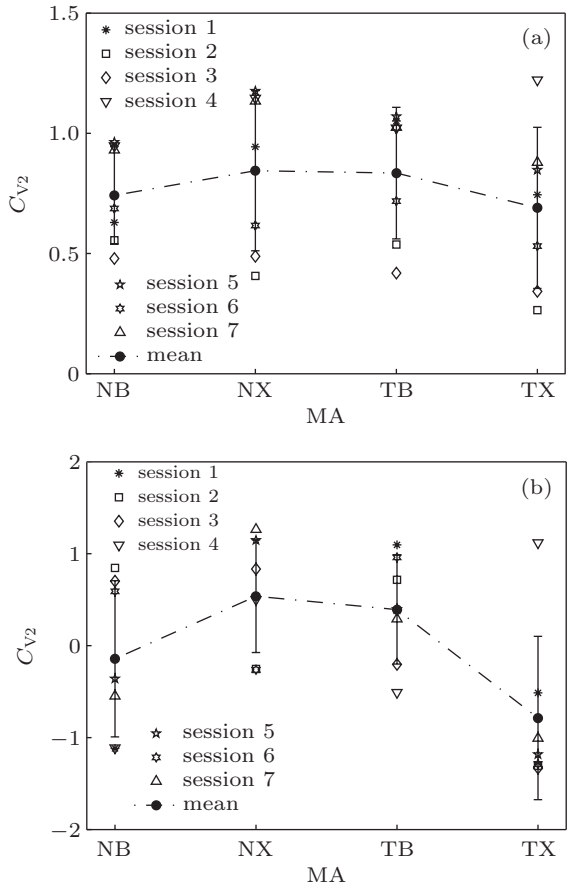


Fig. 8. Statistical analyses of the spiking irregularity measure C_{V2} for the four MA manipulations (7 sessions): (a) original spiking irregularity measure C_{V2}; (b) normalized spiking irregularity measure C_{V2}.

3.5. Measure of spiking irregularity I_R

Recently, another irregularity measure I_R has been proposed and it is also not affected by the rate modulation.[40] It is demonstrated that metric I_R, which measures the instantaneous spiking irregularity similar to L_V, varies in time and with behavioral context.[40] The I_R is defined as follows:

$$I_R = \frac{1}{\ln(4)} \frac{1}{N} \sum_{i=1}^{N} \left| \ln \left(\frac{T_i}{T_{i+1}} \right) \right|, \tag{9}$$

where T_i is an ISI, $|\cdot|$ denotes the absolute value, $I_R = 1$ with the normalization factor $\ln(4)$ for an infinitely long pure Poisson series of events, and $I_R = 0$ for perfectly periodic sequences.[54] The metric I_R applies over the entire time span of two adjacent intervals; however, for computational convenience, it is treated as a point event at the time of the middle spike. Although the numerical simulation of the properties of I_R has been performed by using the intervals generated from a gamma distribution, I_R is independent of the firing rate for ISIs that follow any arbitrary probability distribution.

Figure 9 shows the I_R values of spiking irregularity for the neural activities evoked by four MA manipulations. The NX and TX manipulations can be significantly distinguished. Although the values of NB and TB manipulations are all close to zero, the value of NB is negative and the value of TB is positive. Therefore the NB and TB manipulations can also be distinguished effectively.

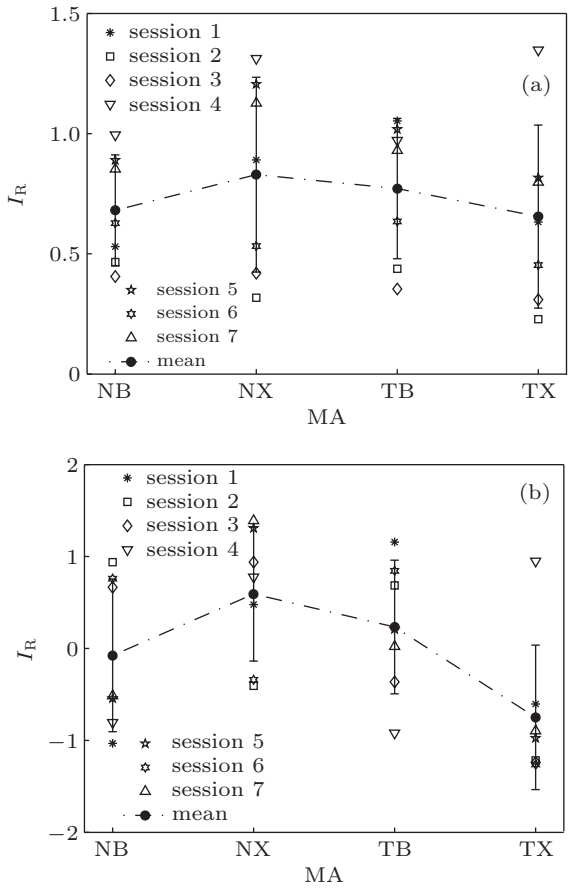


Fig. 9. Statistical analyses of the spiking irregularity measure I_R for the four MA manipulations (7 sessions): (a) original spiking irregularity measure I_R; (b) normalized spiking irregularity measure I_R.

3.6. Statistic analysis of four measures

It is demonstrated in the above five subsections that the ISIH satisfies the gamma distribution and the measures of irregularity, S_I, L_V, and C_{V2}, are related to the shape parameter of the gamma distribution. In addition, compared with C_V, local metrics S_I, L_V, C_{V2}, and I_R, detect firing irregularities fairly invariantly with firing rate fluctuations. Therefore, it is appropriate to use these measures to investigate the ISI sequences evoked by different MA manipulations. It should be noted that our purpose in this paper is not to compare the four measures of irregularity, but to distinguish the MA manipulations by using them together so that various results can be mutually supported.

Figure 10 gives the histograms of the four irregularity measures for the four MA manipulations. Figure 10(a) shows the original spiking irregularity measures and Fig. 10(b) presents the normalized spiking irregularity measures. It can be seen from the figure that each measure has substantially the same statistical histogram distribution for each MA manipulation, i.e., the consistency of the results is verified reciprocally. We can conclude that these four irregularity measures can cor-

rectly and effectively extract the characteristic of acupuncture electrical signals for each MA manipulation.

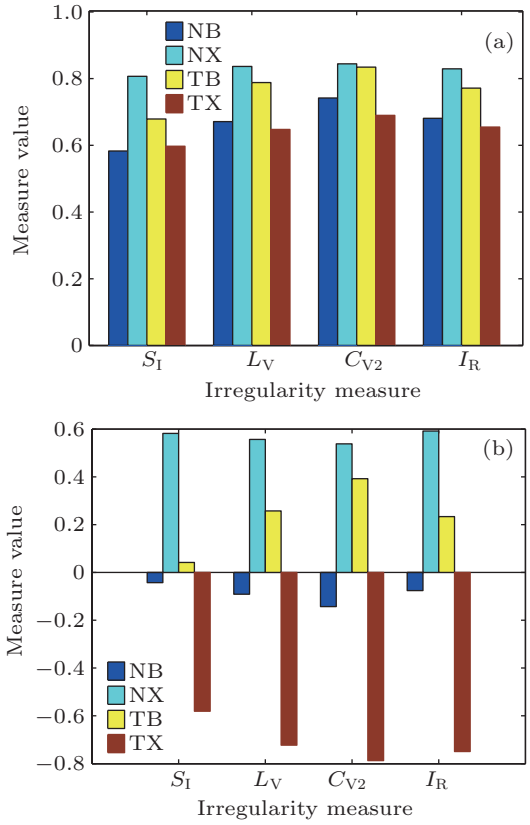


Fig. 10. (color online) Statistical analyses of the four irregularity measures for the four MA manipulations: (a) original spiking irregularity measures; (b) normalized spiking irregularity measures.

Furthermore, the following results of the statistical analysis can be found in Fig. 10(b). The four spiking irregularity measures evoked by NB manipulations distribute in the interval $[-0.2, 0]$. The four spiking irregularity measures evoked by NX manipulations are all close to 0.6, i.e., they have the best consistency. There are big differences between the four spiking irregularity measures evoked by TB manipulations. The four spiking irregularity measures evoked by TX manipulations are distributed in the interval $[-0.8, -0.6]$. The NX and TX manipulations have larger absolute values of the irregularity measures than the NB and TB manipulations. In addition, the irregularity measures of the NB and TX manipulations are negative while the irregularity measures of the NX and TB manipulations are positive. According to the analysis, it can be concluded that differences in irregularity are due to differences in the intrinsic characteristic of MA. Different MA manipulations are related to different spiking irregularity measures. Therefore, the four MA manipulations can be discriminated successfully.

4. Discussion and conclusion

In order to investigate how the MA manipulation modulates the neural system activity, we design an experiment where the MA manipulations are taken at Zusanli in healthy experimental rats and the electrical signals are obtained in the spinal dorsal root ganglion. To quantify the acupuncture effects, we adopt a statistical model to fit the ISI distributions of the neural electrical signals and compute the relevant spiking irregularity measures of the ISI sequences. We limit our statistical analysis to the gamma-process model. The irregularity is easy to determine by using one parameter, i.e., the shape parameter that characterizes the spread of the gamma distribution. The measurement of the irregularity of spike activity is important since it represents the coding capacity per spike.

In this paper, it is shown that different MA manipulations can be distinguished from each other according to the spiking irregularity measures. These results imply that different acupuncture effects possess different coding features. Therefore, based on the new perspective of the statistical model and the irregularity measures, we could further understand the acupuncture and differentiate features of different MA manipulations. The quantitative analysis of acupuncture signals can be further used to make MA more standardized, which can provide a new perspective and method for traditional Chinese acupuncture analysis.

References

[1] Andersson S and Lundeberg T 1995 *Med. Hypotheses* **45** 271
[2] VanderPloeg K and Yi X 2009 *J. Acupunct. Meridian Stud.* **2** 26
[3] Leake R and Broderick J E 1999 *Integr. Med.* **1** 107
[4] Manheimer E, White A, Berman B, Forys K and Ernst E 2005 *Ann. Intern. Med.* **142** 651
[5] Ezzo J, Berman B, Hadhazy V A, Jadad A R, Lao L and Singh B B 2000 *Pain* **86** 217
[6] Ernst E, Lee M S and Choi T Y 2011 *Pain* **152** 755
[7] Lee A and Fan L T 2009 *Cochrane Database of Systematic Reviews* **2** CD003281
[8] Foster J M and Sweeney B P 1987 *Br. J. Hosp. Med.* **38** 308
[9] Tang D A 1987 *Zhen Ci Yan Jiu* **12** 278
[10] Cho Z H, Chung S C, Jones J P, Park J B, Park H J, Lee H J, Wong E K and Min B I 1998 *Proc. Natl. Acad. Sci. USA* **95** 2670
[11] Zhang Y, Qin W, Liu P, Tian J, Liang J M, Karen V D and Liu Y J 2009 *Neurosci. Lett.* **449** 6
[12] Zhang W T, Jin Z and Cui G H 2003 *Brain Res.* **982** 168
[13] Wang T T, Yuan Y, Kang Y, Yuan W L, Zhang H T, Wu L Y and Feng Z T 2005 *Neurosci. Lett.* **382** 236
[14] Han J S 2003 *Trends Neurosci.* **26** 17
[15] Cui Y M and Qi L J 1998 *International Journal of Clinical Acupuncture* **9** 317
[16] Cai W Y 1992 *American Journal of Chinese Medicine* **20** 331
[17] Squire L, Berg D, Bloem F, Lac S D, Ghosh A and Spitzer N 2009 *Sensory System and Motor System* (Beijing: Science Press)
[18] Wang J, Sun L, Fei X and Zhu B 2007 *Chaos Soliton. Fract.* **33** 901
[19] Han C X, Wang J, Che Y Q, Deng B, Guo Y, Guo Y M and Liu Y Y 2010 *Acta Phys. Sin.* **59** 5880 (in Chinese)
[20] Men C, Wang J, Qin Y M, Deng B and Wei X L 2011 *Computer Methods and Programs in Biomedicine* **104** 498
[21] Men C, Wang J, Deng B, Wei X L, Che Y Q and Han C X 2012 *Neurocomputing* **79** 12
[22] Men C, Wang J, Qin Y M, Tsang K M and Deng B 2011 *Applied Mathematical Modelling* **36** 4742
[23] Bian H R, Wang J, Deng B, Wei X L, Han C X and Che Y Q 2011 *Acta Phys. Sin.* **60** 118701 (in Chinese)
[24] Luo X L, Wang J, Han C X, Deng B, Wei X L and Bian H R 2012 *Chin. Phys. B* **21** 028701

[25] Yi G S, Wang J, Han C X, Deng B, Wei X L and Li N 2013 *Chin. Phys. B* **22** 028702
[26] Yi G S, Wang J, Deng B, Wei X L and Han C X 2013 *Chin. Phys. B* **22** 028703
[27] Song Y L 2010 *Acta Phys. Sin.* **59** 2334 (in Chinese)
[28] Gao Z Y and Lu Q S 2007 *Chin. Phys.* **16** 2479
[29] Men C, Wang J, Qin Y M, Wei X L, Che Y Q and Deng B 2011 *Chin. Phys. B* **20** 128704
[30] Shi X and Lu Q S 2005 *Chin. Phys.* **14** 77
[31] Wang H X, Lu Q S and Shi X 2010 *Chin. Phys. B* **19** 060509
[32] Gerstein G and Mandelbrot B 1964 *Biophys. J.* **1** 1
[33] Baker S and Lemon R 2000 *Journal of Neurophysiology* **84** 1770
[34] Tuckwell H 1988 *Introduction to Theoretical Neurobiology: vol. 2, Nonlinear and Stochastic Theories* (Cambridge: Cambridge University Press)
[35] Burns B and Webb A 1976 *Proc. Royal Soc. London B* **194** 211
[36] Miura K, Okada M and Amari M 2006 *Neural Computation* **18** 2359
[37] Christodoulou C and Bugmann G 2001 *Neurocomputing* **38** 1141
[38] Stevens C F and Zador A M 1998 *Nature Neuroscience* **1** 210
[39] Nawrot M, Boucsein C, Rodriguez Molina V, Riehle A, Aertsen A and Rotter S 2008 *Journal of Neuroscience Methods* **169** 374
[40] Davies R M, Gerstein G L and Baker N 2006 *Journal of Neurophysiology* **96** 906
[41] Mainen Z F and Sejnowski T J 1995 *Science* **268** 1503
[42] Ponce-Alvarez A, Kilavik Bjørg E and Riehle A 2009 *Journal of Computational Neuroscience* **29** 351
[43] Shinomoto S, Miura K and Koyama S 2005 *Bio. Systems* **79** 67
[44] Shinomoto S, Miyazaki Y, Tamura H and Fujita I 2005 *Journal of Neurophysiology* **94** 567
[45] Shinomoto S, Shima K and Tanji K 2003 *Neural Computation* **15** 2823
[46] Holt G R, Softky W R, Koch C and Douglas R J 1996 *Journal of Neurophysiology* **75** 1806
[47] Quiroga R Q, Nadasdy Z and Ben-Shaul Y 2004 *Neural Comput.* **16** 1661
[48] Bhumbra G and Dyball R E J 2004 *J. Physiol* **555** 291
[49] Stein R B 1965 *Biophysical Journal* **5** 173
[50] Teich M C, Heneghan C, Lowen S B, Ozaki T and Kaplan E 1997 *Journal of the Optical Society of America* **14** 529
[51] Kuffler S W, Fitzhugh R and Barlow H B 1957 *Journal of General Physiology* **40** 683
[52] Berger T and Levy W B 2009 *Proc. IEEE ISIT* 1584
[53] Shadlen M N and Newsome W T 1998 *Journal of Neuroscience* **18** 3870
[54] Fujiwara K and Aihara K 2009 *Eur. Phys. J. B* **68** 283